Characterization of $(Fe'_{Zr,Ti} - V_O^{\bullet\bullet})^{\bullet}$ Defect Dipoles in (La,Fe)-Codoped PZT 52.5/47.5 Piezoelectric Ceramics by Multifrequency Electron Paramagnetic Resonance Spectroscopy

Emre Erdem, Rüdiger-A. Eichel, Hans Kungl, Michael J. Hoffmann, Andrew Ozarowski, Johan van Tol, and Louis Claude Brunel

***Abstract*—Ferroelectric 1 mol.% La^{3+} and 0.5 mol.% Fe^{3+} codoped $Pb[Zr_{0.54}Ti_{0.46}]O_3$ ceramics were studied by means of multifrequency electron paramagnetic resonance (EPR) spectroscopy. The obtained results prove that iron is incorporated at the [Zr,Ti]-site, acting as an acceptor and building a charged $(Fe'_{Zr,Ti} - V_O^{\bullet\bullet})^{\bullet}$ defect dipole with a directly coordinated oxygen vacancy for partial charge compensation. This feature of the defect associates has hitherto been identified only in hard, exclusively Fe^{3+}-doped PZT compounds. The present results show, however, that a similar defect association of the Fe^{3+} functional center with a $V_O^{\bullet\bullet}$ also exists in soft, donor-acceptor (La^{3+},Fe^{3+})-codoped PZT.**

According to models developed by Arlt *et al.* electric dipoles from defect associates, such as the $(Fe'_{Zr,Ti} - V_O^{\bullet\bullet})^{\bullet}$ defect associate, which may give rise to an internal bias field that is discussed being responsible for ferroelectric aging.

I. Introduction

The characterization of defect structure in piezoelectric lead zirconate titanate $Pb[Zr_xTi_{1-x}]O_3$, (PZT x/1-x) ceramic compounds is an important issue. In particular, acceptor-doped ceramics with high concentration of oxygen vacancies ($V_O^{\bullet\bullet}$) show increased change of their electrical properties with time, the phenomenon being termed as *ferroelectric aging* [1]. On the other hand, donor-doped ceramics with no significant $V_O^{\bullet\bullet}$ concentration are more stable in time concerning their electrical properties [2]. By simultaneously codoping with acceptor- and donor-dopants, PZT compounds of excellent piezoelectric characteristics may be obtained [3]. The common understanding of the aging phenomenon is that domain-wall motion is increasingly restricted with time [4]. Macroscopically, aging is typically indicated by a shift of the hysteresis loop along the electric field axis [5], [6]. This shift is generally termed *internal bias field* and is believed to occur owing to a persistent alignment of defect dipoles present in the material [7]. Obviously, there is major interest to clarify the role of dopant impurities, as well as their immediate surroundings and possible association with lattice vacancies.

In order to microscopically analyze the defect structure, electron paramagnetic resonance (EPR) spectroscopy provides valuable insights [8], [9]. For model-type acceptor-doped hard components, the predicted existence of defect dipoles has been observed for Fe^{3+}-modified $PbTiO_3$ [10]–[12] and $PbZrO_3$ [12], [13] compounds. However, for other acceptor centers, such as Cr^{3+} in $PbTiO_3$ [14] or Cu^{2+} in PZT 54/46 [12], [15], [16], no defect associates were detected up to now.

In this work, we report on multifrequency EPR studies of the Fe^{3+} functional centers in soft (La,Fe)-codoped PZT 52.5/47.5, studied at a temperature of 10 K. The electronic fine-structure (FS) interaction induced by the crystal field originating from the nearest-neighbor O^{2-} ions and potentially oxygen vacancies around the Fe^{3+} center provides the possibility for sensitively probing the local symmetry at the dopant site. Here, we aim particularly to transfer the results obtained for the acceptor-doped hard pure-member phases lead titanate and lead zirconate to a technologically relevant codoped soft PZT composition.

II. Experimental

A. Sample Preparation and Characterization

Stoichiometry calculation for the preparation of the (La,Fe)-codoped PZT 52.5/47.5 powder was based on the assumptions that La^{3+} ions occupy ABO_3 perovskite A^{2+}-sites in the PZT lattice, and that the resulting charge compensation is accomplished by the formation of lead vacancies V''_{Pb}. Fe^{3+} was expected to incorporate to the B^{4+}-site of the perovskite structure. The resulting deficiency in positive charges from iron ions was supposed to be compensated by oxygen vacancies $V_O^{\bullet\bullet}$. Indepen-

Manuscript received May 27, 2007; accepted October 19, 2007.

E. Erdem and R.-A. Eichel are with Eduard-Zintl-Institute, Darmstadt University of Technology, D-64287 Darmstadt, Germany (e-mail: eichel@chemie.tu-darmstadt.de).

H. Kungl and M. J. Hoffmann are with the Institute of Ceramics in Mechanical Engineering, University of Karlsruhe, D-76131 Karlsruhe, Germany.

A. Ozarowski, H. van Tol, and L. C. Brunel are with the Center for Interdisciplinary Magnetic Resonance, National High Magnetic Field Laboratory, Florida State University, Tallahassee, FL 32310.

Digital Object Identifier 10.1109/TUFFC.2008.757

dent formation of V''_{Pb} and $V_O^{\bullet\bullet}$ was assumed. The effects from dopants and the resulting formation of vacancies were taken into account when determining the appropriate amounts of raw materials. Consequently, a powder mixture was prepared according to the chemical composition $Pb_{0.985}La_{0.01}(Zr_{0.5224}Ti_{0.4726}Fe_{0.005})O_{2.9975}$.

The material was prepared by the mixed-oxide route [17]. A detailed description of processing method, processing parameters, and raw materials is given in [18]. After dry forming by uniaxial and subsequent cold isostatical pressing, the pellets were sintered in closed alumina crucibles for 6 hours at 1050°C in air. Mass losses during sintering were at 0.2 wt.% approximately. Densities of the sintered ceramics were at 7.8 g cm^{-3}. The samples for the EPR measurements were prepared from slices, which were cut from the inner part of the sintered bodies. The slices were first ground and polished to a thickness of 250 μm. Thereafter, rectangular plates were sawed from these thin ceramic disks. For the W-band experiments $6 \times 6 \times 0.25$ mm^3 plates were used. Dimensions of the samples prepared for the X- and Q-band measurements were $4 \times 6 \times 0.25$ mm^3.

B. Spectroscopic Measurements

X- (9.4 GHz) and Q-band (34 GHz) band continuous wave EPR measurements were performed on Bruker ESP 300E spectrometers with rectangular TE_{112} and cylindrical dielectric TE_{102} resonators, respectively. The magnetic field was read out with an NMR gaussmeter (ER 035M, Bruker AG, Karlsruhe, Germany) and for cryogenic temperatures down to 10 K, a helium-flow cryostat (Oxford Instruments, Oxford, UK) was used. The applied microwave power was $1.0 \cdot 10^{-3}$ mW, and the field was modulated with a frequency of 100 kHz and amplitude of 0.1 mT. The magnetic field was calibrated by a standard field marker (polycrystalline DPPH with $g = 2.0036$).

Field-modulated continuous wave EPR experiments at high-frequencies (107.2 GHz) were performed at the high-magnetic field facility at the National High Magnetic Field Laboratory, using a quartz synthesizer for the microwave (mw) radiation and a setup without resonator [19].

III. Theoretical Description

A. Electron Paramagnetic Resonance

The trivalent lanthanum ion has a $5p^6$ electronic configuration, hence being diamagnetic and consequently not showing any EPR signal. Contrary, the free trivalent iron ion possesses five unpaired electrons in the $3d$ shell ($3d^5$) with a high-spin $^6S_{5/2}$ ground state. The corresponding spin-Hamiltonian for this ion may be written as:

$$\mathcal{H} = g_{iso}\beta_e \mathbf{B_0} \cdot \mathbf{S} + \sum_{k=2,\ldots,6}^{-k \le q \le k} B_k^q \, O_k^q(S_x, S_y, S_z), \quad (1)$$

where the g-matrix may be replaced by an isotropic value $g_{iso} = 2.002$, β_e denotes the Bohr magneton, $\mathbf{B_0}$ the external magnetic field, B_k^q are the FS spin-Hamiltonian parameters, and O_k^q are the extended Stevens spin operators [20], [21]. In principle, all conceivable B_k^q parameters, resulting from 2nd to 6th-rank tensors, have to be considered [22]. However, experimentally only the 2nd-rank B_2^q parameters for Fe^{3+} could reliably be determined by means of numerical spectrum simulation using (1).

B. Newman Superposition-Model Analysis

In order to extract relevant structural information from the obtained Fe^{3+} FS parameters, the B_2^q spin-Hamiltonian parameters for different oxygen octahedral arrangements about the Fe^{3+} functional center may be modeled by summing up contributions from particular ligands. In the case of the Fe^{3+} functional center in PZT, these contributions are generated predominantly from the nearest-neighbor oxygen-ligand surrounding. According to the Newman superposition model (NSM), the B_2^q FS parameters can be expressed as sum over the single oxygen ligands [23]:

$$B_2^q = \frac{1}{3} \sum_i \bar{b}_2(R_i) K_2^q(\theta_i, \phi_i), \quad (2)$$

with the single-ligand contribution $\bar{b}_2(R_i)$ obeying a power-law dependence on the distance between the Fe^{3+} and O^{2-} ions according to:

$$\bar{b}_2(R_i) = \bar{b}_2(R_0) \left(\frac{R_0}{R_i} \right)^{t_2}. \quad (3)$$

The coordination factors $K_2^q(\theta_i, \phi_i)$ embody the geometrical arrangement of the ligand oxygens [24], [25]. The power-law exponent t_2 together with the single-ligand contribution $\bar{b}_2(R_0)$, where R_0 corresponds to the intrinsic $Fe^{3+} - O^{2-}$ bond distance. They are characteristic for the particular ion-ligand system and have been refined empirically over the last decades.

In order to include a $V_O^{\bullet\bullet}$ at a particular oxygen site into the modeling of B_2^q, the corresponding term in (2) is set to zero.

IV. Results

A. Multifrequency-EPR Analysis

The X-band EPR spectrum of soft (La^{3+},Fe^{3+})-codoped PZT 52.5/47.5 is depicted in Fig. 1(a). Analogously to the recently reported EPR analysis of (La^{3+},Fe^{3+})-codoped PZT 40/60 [18], the observed X-band spectra are representative for the so-termed low-frequency regime ($3B_2^q \gg h\nu_{mw}$) with two main resonances at low fields. Principally, these give information about the prevailing Fe^{3+} site symmetry. The resonance at 120 mT is representative for a center of tetragonal symmetry and

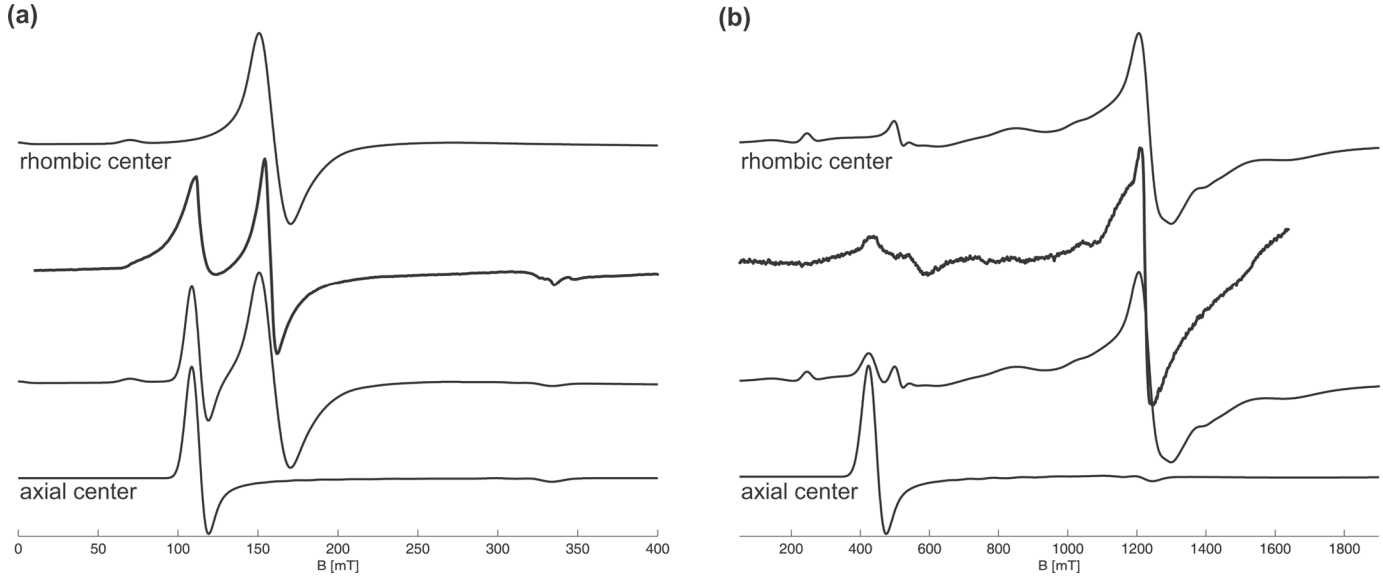

Fig. 1. (a) X- (9.4 GHz) and (b) Q-band (34 GHz) EPR spectra of 1.0 mol% La^{3+}, 0.5 mol% Fe^{3+}-doped PZT 52.5/47.5 at 10 K. Numerical spectrum simulations are superimposed to the experimental spectra, visualizing the contribution of rhombic (top) and axial (bottom) centers to the EPR spectrum.

the resonance at 180 mT is due to a center of rhombic symmetry. Even though, in the low-frequency regime the symmetry of the FS tensor may sensitively be determined, no further information is accessible about the sign and size of the FS parameters.

By increasing the Larmor frequency to Q-band (34 GHz) an intermediate-frequency regime ($3B_2^q \approx h\nu_{\mathrm{mw}}$) is established for the rhombic center. In the corresponding EPR spectrum, given in Fig. 1(b), spectral contributions from the two centers are separated as the axial center still is in the low-frequency regime, for which reason only a resonance line at 500 mT is observed. The remaining resonances are due to the rhombic center. The situation is complicated because so-called looping transitions that do not continue over all possible orientations, and crossing transitions that are degenerate at specific orientations occur [26]. Hence, the determination of FS parameters is facilitated only by numerical spectrum simulation.

In order to extract also the FS parameters for the axial center, again the mw frequency is selectively chosen so that this center is in the intermediate-frequency regime. For the rhombic center, the high-frequency regime ($3B_2^q \ll h\nu_{\mathrm{mw}}$) is established. This situation is achieved by going to even higher Larmor frequencies at W-band (107.2 GHz). Again, spectral contributions of the two centers do not overlap, because now the resonances originating from the rhombic center are centered about $g = 2.002$ (~ 3.9 T). The resonances from the axial center span the field range down to almost zero field. The corresponding EPR spectrum is shown in Fig. 2. Additionally to the size of the FS parameters, at low temperatures their sign may be determined.

By using multifrequency EPR numerical spectrum simulation, the determined results for the Fe^{3+} 2nd-rank FS parameters are summarized in Table I.

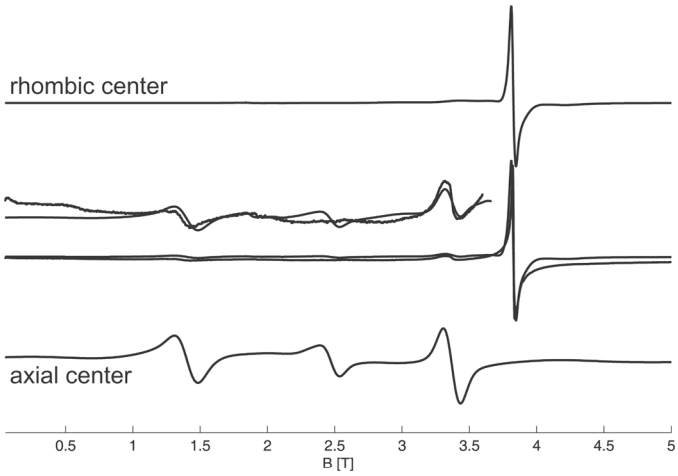

Fig. 2. High-frequency 107.2 GHz EPR spectrum of 1.0 mol% La^{3+}, 0.5 mol% Fe^{3+}-doped PZT 52.5/47.5 at 10 K. Numerical spectrum simulations are superimposed to the experimental spectrum, visualizing the contribution of rhombic (top) and axial (bottom) centers to the EPR spectrum.

TABLE I
SPIN-HAMILTONIAN PARAMETERS FOR THE RHOMBIC AND TETRAGONAL CENTERS IN 1.0 MOL% La^{3+}, 0.5 MOL% Fe^{3+}-DOPED PZT 52.5/47.5 AT 10 K.[1]

	g_{iso}	B_2^0 (GHz)	B_2^2 (GHz)
Rhombic center	2.002	6.5	2.2
Tetragonal center	2.002	12.2	—

[1]Obtained by multifrequency numerical spectrum simulation.

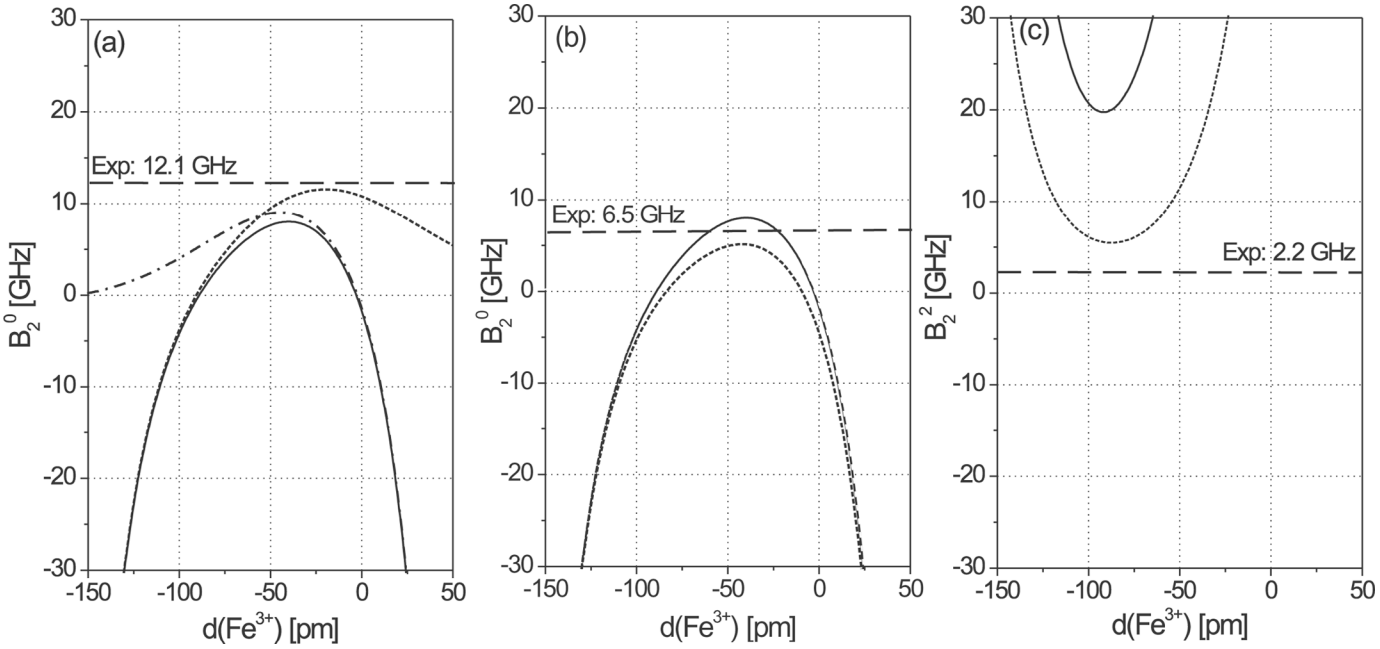

Fig. 3. Newman superposition calculations for B_2^0 (a) and (b) and B_2^2 (c) for (La^{3+},Fe^{3+})-codoped PZT 52.5/47.5. (a) Oxygen vacancy at apical position. (b) and (c) Oxygen vacancy at equatorial position. The dashed horizontal lines represent the experimental values for B_2^0 and B_2^2, respectively. The dashed lines represent the Newman superposition calculations with an associated oxygen vacancy. The solid lines are for calculations assuming a complete octahedron. The distance d is defined according to a line connecting O^{2-} and the original B-site position, with the positive direction toward the O^{2-} position.

B. Superposition-Model Analysis

In order to convert the determined information embodied in the Fe^{3+} FS parameters into structural information, different models concerning the local structure at the Fe^{3+} functional center will be considered with the help of the semi-empirical Newman superposition model [23]. Hereby, the intrinsic NSM parameters $\bar{b}_2 = -12.3514$ GHz, $t_2 = 8$, and $R_0 = 210.1$ pm were adopted from MgO single crystals containing Fe^{3+} impurity centers. This system has equivalent $Fe^{3+}-O^{2-}$ bonds in octahedral coordination [27], [28]. For the modeling of the $(Fe'_{Zr,Ti} - V_O^{\bullet\bullet})^{\bullet}$ centers in $PbTiO_3$ [11] and $PbZrO_3$ [13], respectively, this set of parameters already has proved yielding reliable results. The nearest-neighbor oxygen positions were taken from the X-ray data at ambient temperature [29]. In order to roughly estimate the increased crystallographic c/a-ratio at 10 K as compared to the data reported at ambient temperature, the fractional coordinates along the crystallographic c-axis were increased by 20%. This value seems reasonable as a similar temperature dependence has been observed for $PbTiO_3$ [11]. Owing to the tetragonal crystal symmetry, the coordinate system for the NSM calculation was chosen identical to the crystal coordinate system. The FS tensor was transformed into its eigenframe.

In order to decide if an oxygen vacancy occurs in the first coordination sphere of the iron center or if charge compensation occurs in a more distant sphere, structural models were investigated with and without an oxygen vacancy in the nearest neighbor position of the Fe^{3+} center. Additionally, for the model assuming a $(Fe'_{Zr,Ti} - V_O^{\bullet\bullet})^{\bullet}$ defect association, two different arrangements were considered, accounting for the observed centers of tetragonal and rhombic symmetry. Consequently, the $V_O^{\bullet\bullet}$ was once located at the apical oxygen position, and then at the equatorial one. Parameters B_2^0 and B_2^2 then were calculated varying the position of Fe^{3+} ion along the line connecting its initial position with the respective oxygen position, in which the distance d is defined as the shift of the Fe^{3+} ion along this line. Within this convention, a positive sign of d denotes a shift toward the oxygen vacancy.

Fig. 3 represents the calculated FS parameters B_2^0 and B_2^2 as functions of the distance d for the three structural models. For comparison, the experimentally-obtained values for B_2^0 and B_2^2 are represented by solid horizontal lines for both the axial and the rhombic center. Obviously, considering the results obtained for the axial center [Fig. 3(a)], agreement with the experimentally obtained B_2^0 value can be obtained only if an $(Fe'_{Zr,Ti} - V_O^{\bullet\bullet})^{\bullet}$ defect associate is generated as the model invoking a complete octahedron does not reproduce the experimental value regardless of displacement d. Exploiting the so determined displacement parameter d for the axial center, a microscopic arrangement emerges in which the Fe^{3+} functional center relaxes back into the plane of equatorial oxygens. This observation is in qualitative agreement with the results obtained for acceptor-type Fe^{3+}-modified $PbTiO_3$ [11].

When considering the rhombic center [Fig. 3(b)], in principle, also the situation with complete oxygen octahedron reproduces the experimentally B_2^0 value. However, in this arrangement, a tetragonal site symmetry would result contradicting the symmetry as determined by the multi-

frequency EPR analysis. Furthermore, the results obtained for the B_2^2 value [Fig. 3(c)] are clearly in favor of the proposed $(Fe'_{Zr,Ti} - V_O^{\bullet\bullet})^{\bullet}$ defect association.

With respect to the reliability of the predictions obtained by the semi-empirical NSM approach, the arguments pointed out in former studies should be taken into account [11], [13]. These include the fact that crystal distortions near the substituted ion and contributions from ions or vacancies more distant than neighboring ligands are neglected, the assumption made in the NSM analysis that the spin-Hamiltonian parameters exclusively result from individual crystal field contributions of every nearest-neighbor ion, and the approximation of two-electron expectation values characteristic for the FS interaction by means of single-electron-derived charge densities. Because the NSM has proved to yield reliable results for determining the second-rank FS parameters in S-state ions, owing to a continuous refinement of its intrinsic parameters over several decades using a large set of experimental data, the here predicted structural data is considered as reliable.

V. Discussion

Concerning the prevailing defect-structural arrangement at the Fe^{3+} functional center site, the Fe^{3+} ion is incorporated onto the perovskite B-site, acting as an acceptor. For partial charge compensation, $(Fe'_{Zr,Ti} - V_O^{\bullet\bullet})^{\bullet}$ defect dipoles are created. Concerning the resulting displacements of the $Fe'_{Zr,Ti}$ center as compared to the $Zr_{Zr}^{\times}$ and $Ti_{Ti}^{\times}$ positions, the B_2^0 calculations predict a displacement d of the Fe^{3+} functional center in opposite directions of the oxygen vacancy toward the remaining pyramid of oxygen ions. Qualitatively, this result corresponds to the situations encountered in Fe^{3+}-doped hard $PbTiO_3$ [11] and $PbZrO_3$ [13], for which a comparable relaxation of the Fe^{3+} functional center back into the plane of the equatorial oxygens has been observed. Consequently, the size of the corresponding defect dipole moment is enhanced because the distance between $V_O^{\bullet\bullet}$ and $Fe'_{Zr,Ti}$ is increased.

A particularly interesting observation is that the Fe^{3+} functional center is still associated with a charge compensating $V_O^{\bullet\bullet}$, even though the compound investigated is a soft donor-doped material by majority. For such cases, it has been discussed that the V''_{Pb} may compensate the $V_O^{\bullet\bullet}$ resulting in reduced concentrations of both types of vacancies. However, the formation of $(Fe'_{Zr,Ti} - V_O^{\bullet\bullet})^{\bullet}$ defect associates seems to be favored over a complete compensation in case of (La^{3+},Fe^{3+})-codoped PZT 52.5/47.5. This type of charge compensation has not yet been clarified.

More generally, the $(Fe'_{Zr,Ti} - V_O^{\bullet\bullet})^{\bullet}$ defect dipole provides an anisotropic center that favors a specific direction of polarization. It has been much speculated about the orientation of the $(Fe'_{Zr,Ti} - V_O^{\bullet\bullet})^{\bullet}$ defect dipole with respect to the orientation of the spontaneous polarization [30]. In (La^{3+},Fe^{3+})-codoped PZT 52.5/47.5, two types of $(Fe'_{Zr,Ti} - V_O^{\bullet\bullet})^{\bullet}$ centers were observed, which differ with respect to their orientation relative to the direction of spontaneous polarization. Both arrangements of the corresponding defect dipole, parallel and perpendicular to the orientation of spontaneous polarization, were found. In this scenario, the orientation of the defect dipoles are defined by the position of the oxygen vacancy in the oxygen octahedron. A $V_O^{\bullet\bullet}$ in one of the equatorial oxygen positions generates a $(Fe'_{Zr,Ti} - V_O^{\bullet\bullet})^{\bullet}$ defect dipole perpendicular to the orientation of spontaneous polarization. A $V_O^{\bullet\bullet}$ in the apical oxygen positions forms a defect dipole collinear to the orientation of spontaneous polarization. Changes in the position of the $V_O^{\bullet\bullet}$ within the oxygen octahedron via ionic hopping processes will result in a reorientation of the corresponding dipole. The kinetic behavior of a situation in which an oxygen vacancy is a mobile particle in the oxygen octahedron enclosing an acceptor ion has been described in a relaxation model [30]. Within this model, the relaxation time of ferroelectric ceramics is determined by the thermally activated diffusive jumping of the oxygen vacancies.

More generally, macroscopic dielectric and ferroelectric properties of PZT strongly depend on the prevailing microscopic defect structure [7], [31]–[33]. With this respect, the macroscopic behavior of aged ferroelectric materials, in particular the shift of the polarization hysteresis loops along the electric field axis, is attributed to effects resulting from the presence of point defects. This macroscopic phenomenon is known as internal bias field. However, there are different approaches for the explanation of the underlying physical origin of an internal bias field and its interaction with point defects [34]. On the one-hand, domain walls can be pinned at positions of low energy, such as provided by point defects. The pinning may either occur if the domain wall moves toward a point defect [35], [36] or by migration of the point defect toward the domain wall [37]. Alternatively, it has been proposed that the internal bias field is due to internal electric dipoles resulting from a cooperative mechanism such as an alignment of defect associates along a persistent orientation. This mechanism was investigated in detail for Ni^{2+}-doped $BaTiO_3$ [30]. The possibility that dipolar defect complexes can pin the polarization of the surrounding crystal has been furthermore demonstrated by density functional theory (DFT) calculations [38]. In particular, oxygen-vacancy related defect dipoles have been shown to be involved in voltage offsets leading to imprint failure [39] and are suggested to play a crucial role in electrical fatigue [38], [40]. Moreover, an alignment of the defect dipoles leads to an increased internal bias field that may lead to a clamping of domain walls [41]. The defect-structural arrangements found here, including directions of internal bias fields and spontaneous polarization, are schematically illustrated in Fig. 4.

The ferroelectric aging phenomenon in ABO_3 perovskite oxides containing a defect structure consisting of a $V_O^{\bullet\bullet}$ and an acceptor impurity D'_B has also theoretically been considered in detail [42]. The probability of finding an oxygen vacancy in the nearest neighbor position of the D'_B acceptor center is predicted to be highest along the crystallographic c-axis. In this symmetry-conforming point

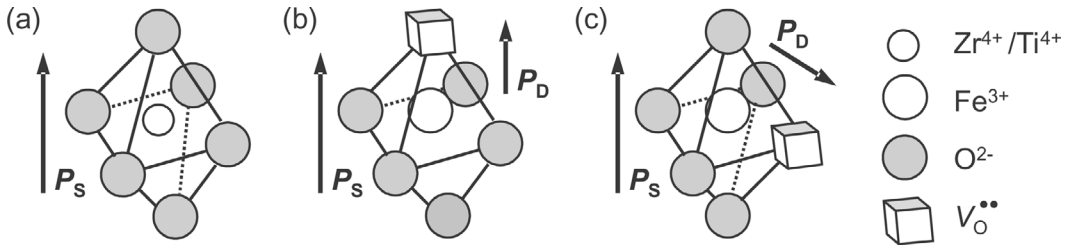

Fig. 4. Schematic representation of the proposed structural models. (a) Zr^{4+}, Ti^{4+} sites surrounded by an oxygen octahedron, as representative for the situation in the undoped compound. (b) $(Fe'_{Zr,Ti} - V_O^{\bullet\bullet})^{\bullet}$ defect dipole oriented along the crystallographic c-axis, forming an axial center. (c) $(Fe'_{Zr,Ti} - V_O^{\bullet\bullet})^{\bullet}$ defect dipole oriented along the crystallographic a, b-axes, creating a rhombic center. The directions for spontaneous polarization (P_S) and defect polarization (P_D) are indicated by arrows.

defect configuration, the spontaneous polarization associated with the polar tetragonal crystal symmetry, and the defect polarization, associated with the noncentric distribution of charged point defects, are oriented in antiparallel with respect to each other. As a consequence, the nonreversible domain switching in aged ferroelectrics was proposed due to such symmetry-conforming point defects. In this model, the orientation of defect dipoles was shown to be unstable in the cubic paraelectric phase. In a tetragonal ferroelectric phase, they were transformed to a stable state after aging. The defect symmetry followed the crystal symmetry. A similar model already has been proposed on the basis of a gradual alignment of $(Fe'_{Ti} - V_O^{\bullet\bullet})^{\bullet}$ defect dipoles in $BaTiO_3$ and PZT [43], [44].

VI. Conclusions

The existence of $(Fe'_{Zr,Ti} - V_O^{\bullet\bullet})^{\bullet}$ defect dipoles in (La^{3+},Fe^{3+}) co-doped PZT 52.5/47.5 has been experimentally observed by means of a multifrequency EPR study. In particular, the approach presented here may allow one to further investigate the interplay between defect dipoles with respect to the macroscopic phenomena, such as the poling behavior, the ferroelectric aging, or the existence of internal bias fields also in soft-doped material. Macroscopically, their existence may lead to internal bias fields.

Acknowledgments

This research has been financially supported by the DFG Centre of Excellence 595, *Electrical Fatigue in Functional Materials*. The authors are grateful to Prof. Dr. K.-P. Dinse for allowing the use of an X-band continuous-wave EPR spectrometer in his lab. Furthermore, the authors would like to thank Mrs. Edeltraud Vogel (IKM Karlsruhe) for the careful machining of the 250-μm ceramic slices.

References

[1] P. V. Lambeck and G. H. Jonker, "The nature of domain stabilization in ferroelectric perovskites," *J. Phys. Chem. Solids*, vol. 47, pp. 453–461, 1986.

[2] B. Jaffe, W. R. Cook, and H. Jaffe, *Piezoelectric Ceramics*. London: Academic Press, 1971.

[3] M. J. Hoffmann and H. Kungl, "High strain lead-based perovskite ferroelectrics," *Curr. Op. Solid State Mat. Sci.*, vol. 8, pp. 51–57, 2004.

[4] H. Neumann and G. Arlt, "Dipole orientation in Cr-modified $BaTiO_3$ ceramics," *Ferroelectrics*, vol. 76, pp. 303–310, 1987.

[5] K. Carl and K. H. Härdtl, "Electrical after effects in $Pb(Ti,Zr)O_3$ ceramics," *Ferroelectrics*, vol. 17, p. 473, 1978.

[6] S. Takahashi, "Effects of impurity doping in lead zirconate-titanate ceramics," *Ferroelectrics*, vol. 41, p. 143, 1982.

[7] G. Arlt and H. Neumann, "The role of domain walls on the dielectric, elastic and piezoelectric properties of ferroelectric ceramics," *Ferroelectrics*, vol. 76, p. 451, 1987.

[8] R.-A. Eichel, "Defect structure of oxide ferroelectrics—Valence state, site of incorporation, mechanisms of charge compensation and internal bias fields," *J. Electroceram.*, vol. 19, pp. 9–21, 2007.

[9] R.-A. Eichel, "Characterization of defect structure in acceptor-modified piezoelectric ceramics by multifrequency and multipulse electron paramagnetic resonance spectroscopy," *J. Am. Ceram. Soc.*, vol. 91, pp. 691–701, 2008.

[10] H. Meštrić, R.-A. Eichel, K.-P. Dinse, A. Ozarowski, J. van Tol, and L. C. Brunel, "High-frequency electron paramagnetic resonance investigation of the Fe^{3+} impurity center in polycrystalline $PbTiO_3$ in its ferroelectric phase," *J. Appl. Phys.*, vol. 96, pp. 7440–7444, 2004.

[11] H. Meštrić, R.-A. Eichel, T. Kloss, K.-P. Dinse, S. Laubach, S. Laubach, and P. C. Schmidt, "Iron-oxygen vacancy defect centers in $PbTiO_3$: Newman superposition model analysis and density functional calculations," *Phys. Rev. B*, vol. 71, art. no. 134109, 2005.

[12] R.-A. Eichel, H. Meštrić, K.-P. Dinse, A. Ozarowski, J. van Tol, L. C. Brunel, H. Kungl, and M. J. Hoffmann, "High-field/high-frequency EPR of paramagnetic functional centers in Cu^{2+}- and Fe^{3+}-modified polycrystalline $Pb[Zr_xTi_{1-x}]O_3$ ferroelectrics," *Magn. Reson. Chem.*, vol. 43, pp. S166–S176, 2005.

[13] H. Meštrić, R.-A. Eichel, K.-P. Dinse, A. Ozarowski, J. van Tol, L. C. Brunel, H. Kungl, M. J. Hoffmann, K. A. Schönau, M. Knapp, and H. Fuess, "Iron-oxygen vacancy defect association in polycrystalline iron-modified $PbZrO_3$ antiferroelectrics: Multifrequency electron paramagnetic resonance and Newman superposition model analysis," *Phys. Rev. B*, vol. 73, art. no. 184105, 2006.

[14] E. Erdem, R. Böttcher, H. C. Semmelhack, H. J. Gläsel, and E. Hartmann, "Multi-frequency EPR studyof Cr^{3+} doped lead titanate ($PbTiO_3$) nanopowders," *Phys. Stat. Sol. (b)*, vol. 239, pp. R7–R9, 2003.

[15] R.-A. Eichel, H. Kungl, and M. J. Hoffmann, "Determination of functional center local environment in copper-modified $Pb[Zr_{0.54}Ti_{0.46}]O_3$ ceramics," *J. Appl. Phys.*, vol. 95, pp. 8092–8096, 2004.

[16] R.-A. Eichel, K.-P. Dinse, H. Kungl, M. J. Hoffmann, A. Ozarowski, J. van Tol, and L. C. Brunel, "Exploring the morphotropic phase boundary in copper(II)-modifed $Pb[Zr_{0.54}Ti_{0.46}]O_3$ ferroelectrics," *Appl. Phys. A*, vol. 80, pp. 51–54, 2005.

[17] M. Hammer and M. J. Hoffmann, "Sintering model for mixed-oxide-derived lead zirconate titanate ceramics," *J. Amer. Ceram. Soc.*, vol. 81, pp. 3277–3284, 1998.
[18] E. Erdem, R.-A. Eichel, H. Kungl, M. J. Hoffmann, A. Ozarowski, H. van Tol, and L. C. Brunel, "Local symmetry-reduction in tetragonal (La,Fe)-codoped $Pb[Zr_{0.4}Ti_{0.6}]O_3$ piezoelectric ceramics," *Physica Scripta*, vol. T129, pp. 12–16, 2007.
[19] J. van Tol, L. C. Brunel, and R. J. Wylde, "A quasioptical transient electron spin resonance spectrometer operating at 120 and 240 GHz," *Rev. Sci. Instrum.*, vol. 76, art. no. 074101, 2005.
[20] A. Abragam and B. Bleaney, *Electron Paramagnetic Resonance of Transition Ions*. Oxford: Clarendon, 1970.
[21] C. Rudowicz, *Magn. Reson. Rev.*, vol. 13, pp. 1–89, 1987.
[22] V. G. Grachev, "Correct expression for generalized spin-Hamiltonian of non-cubic paramagnetic center," *Sov. Phys. JETP*, vol. 65, pp. 1029–1035, 1987.
[23] D. J. Newman and B. Ng, "The superposition model of crystal fields," *Rep. Prog. Phys.*, vol. 52, pp. 699–763, 1989.
[24] S. C. Chen and D. J. Newman, "The orbit-lattice interaction for lanthanide ions: superposition model analysis for arbitrary symmetry," *Aust. J. Phys.*, vol. 35, pp. 133–145, 1982.
[25] C. Rudowicz, "Transformation relations for the conventional and normalised Stevens operator equivalents," *J. Phys. C: Solid State Phys.*, vol. 18, pp. 1415–1430, 1985.
[26] K. S. Misra, "Angular variation of electron paramagnetic resonance spectrum: Simulation of a polycrystalline EPR spectrum," *J. Magn. Res.*, vol. 137, p. 8392, 1999.
[27] E. Siegel and K. A. Müller, "Structure of transition-metal-oxygen-vacancy pair centers," *Phys. Rev. B*, vol. 19, p. 109, 1979.
[28] D. J. Newman and E. Siegel, "Superposition model analysis of Fe^{3+} and Mn^{2+} spin-Hamiltonian parameters," *J. Phys. C*, vol. 9, p. 4285, 1976.
[29] B. Noheda, J. A. Gonzalo, L. E. Cross, R. Guo, S. E. Park, D. E. Cox, and G. Shirane, "Tetragonal-to-monoclinic phase transition in a ferroelectric perovskite: The structure of $Pb[Zr_{0.52}Ti_{0.48}]O_3$," *Phys. Rev. B*, vol. 61, pp. 8687–8695, 2000.
[30] G. Arlt and H. Neumann, "Internal bias in ferroelectric ceramics: Origin and time dependence," *Ferroelectrics*, vol. 87, pp. 109–120, 1988.
[31] G. Arlt and P. Sasko, "Domain configuration and equilibrium size of domains in $BaTiO_3$ ceramics," *J. Appl. Phys.*, vol. 51, p. 4956, 1980.
[32] G. Arlt, D. Hennings, and G. de With, "Dielectric properties of fine-grained barium titanate ceramics," *J. Appl. Phys.*, vol. 58, p. 1619, 1985.
[33] G. Arlt, "Microstructure and domain effects in ferroelectric ceramics," *Ferroelectrics*, vol. 91, pp. 3–7, 1989.
[34] H. Neumann, "Das innere Feld in akzeptor-dotierter Bariumtitanat Keramik," Ph.D. thesis, RWTH - Rheinisch Westfälische Technische Hochschule, Aachen, Germany, 1988.
[35] K. W. Plessner, "Ageing of the dielectric properties of barium titanate ceramics," in *Proc. Phys. Soc.*, vol. 73, 1956, p. 1261.
[36] B. Lewis, in *Proc. Phys. Soc.*, vol. 73, 1960, p. 17.
[37] A. Miserova, "Aging of barium titanate single crystals," *Sol. State Phys.*, vol. 2, p. 1276, 1960.
[38] S. Pöykkö and D. J. Chadi, "Dipolar defect model for fatigue in ferroelectric perovskites," *Phys. Rev. Lett.*, vol. 83, p. 1231, 1999.
[39] G. E. Pike, W. L. Warren, D. Dimos, B. A. Tuttle, R. Ramesh, J. Lee, V. G. Keramidas, and J. T. Evans, "Voltage offsets in $(Pb,La)(Zr,Ti)O_3$ thin films," *Appl. Phys. Lett.*, vol. 66, p. 484, 1995.
[40] A. K. Tagantsev, I. Stolichnov, E. L. Colla, and N. Setter, "Polarization fatigue in ferroelectric films: Basic experimental findings, phenomenological scenarios, and microscopic features," *J. Appl. Phys.*, vol. 90, pp. 1387–1402, 2001.
[41] U. Robels, C. Zadon, and G. Arlt, "Linearization of dielectric nonlinearity by internal bias fields," *Ferroelectrics*, vol. 133, pp. 163–168, 1992.
[42] X. Ren, "Large electric-field-induced strain in ferroelectric crystals by point-defect mediated reversible domain switching," *Nature Mater.*, vol. 3, pp. 91–94, 2004.
[43] W. L. Warren, D. Dimos, G. E. Pike, K. Vanheusden, and R. Ramesh, "Alignment of defect dipoles in polycrystalline ferroelectrics," *Appl. Phys. Lett.*, vol. 67, pp. 1689–1691, 1995.
[44] W. L. Warren, G. E. Pike, K. Vanheusden, D. Dimos, B. A. Tuttle, and J. Robertson, "Defect-dipole alignment and tetragonal strain in ferroelectrics," *J. Appl. Phys.*, vol. 79, pp. 9250–9257, 1996.

Emre Erdem was born in Silifke, Turkey, in 1975. He earned a B.Sc. degree in physics in Ankara University, Ankara, Turkey, and a Ph.D. degree in physics in University of Leipzig, Leipzig, Germany.

He worked as a teaching assistant in University of Ankara (1998–1999) and University of Leipzig (2001–2006). At present he is working as a scientific co-worker in Darmstadt University of Technology, Darmstadt, Germany. His main areas of expertise and research interests lie in defect chemistry and size effects in ferroelectric and ferromagnetic materials. Together with other standard and analytical techniques, electron paramagnetic resonance spectroscopy is the main method that he uses for his research field.

He is the member of the International Electron Paramagnetic Resonance Society.

Rüdiger-A. Eichel is a research associate at the Technical University Darmstadt, Darmstadt, Germany. He earned his diploma in solid-state physics at the University of Cologne, Cologne, Germany, (1998) with a thesis at the Institute for Space Simulation in the German Aerospace Center (DLR) about *Surface Segregation of Binary Undercooled Co-Cu and Co-Fe Alloys*. He obtained his Ph.D. degree in physical chemistry at the Swiss Institute of Technology (ETH) in Zürich (2001) about *New Concepts in 2D Pulse EPR*. After a post-doctoral stay at the UC Berkeley, Berkeley, CA, (2001), he joined the Technical University in Darmstadt as a project leader. In 2005 he submitted his habilitation thesis, *Nanoscale Properties of Functional Ceramics Probed by EPR*, and has been awarded Privatdozent in 2006.

Dr. Eichel is a member of the Deutsche Physikalische Gesellschaft and the European Physical Society, as well as the International EPR Society, the Deutsche Bunsengesellschaft, and the Fachgruppe Magnetische Resonanz of the Gesellschaft Deutscher Chemiker. Current research interests include the physics of nanostructures and the defect-chemistry in modified oxide ceramics.

Hans Kungl studied mechanical engineering with a focus on turbomachinery at the University of Karlsruhe, Karlsruhe, Germany, where he received the diploma in 1999. After 2 years working in a project on thermal barrier coatings at the Insitute of Ceramics in Mechanical Engineering (IKM) in Karlsruhe, he joined the ferroelectrics group at this facility. In 2005 he received his Ph.D. degree from the University of Karlsruhe for a thesis on strain behavior of morphotropic PZT.

Presently he is working as a post doc on DC fatigue of PZT. Dr. Kungl is a member of the American Ceramic Society. His major research topics are processing of ferroelectric materials and strain mechanisms in PZT.

Michael J. Hoffmann is professor of ceramic materials and systems in the department of mechanical engineering at the University of Karlsruhe, Karlsruhe, Germany. He earned his diploma in technical mineralogy from the Technical University of Darmstadt, Darmstadt, Germany, (1985) and his Ph.D. degree in chemistry from Universität Stuttgart, Stuttgart, Germany (1989). Before he joined the University of Karlsruhe as a professor and managing director of the Institute of Ceramics for Mechanical Engineering, he was a researcher at the Max-Planck-Institut für Metallforschung in Stuttgart from 1985–1995.

His research activities are focused on nonoxide structural ceramics as well as on ferroelectric ceramics. He received the Masing-Gedächnispreis of Deutschen Gesellschaft für Materialkunde (1993) and the Dionýz Ilkovič Memorial Medal of the Slovak Academy of Sciences (2003). He is a member of the World Academy of Ceramics (2005) as well as a Fellow of the American Ceramic Society (2006). He has published over 100 technical papers and holds several patents.

Andrzej Ozarowski is an assistant in research at the National High Magnetic Field Laboratory, Tallahassee, FL. He earned his Ph.D. degree in chemistry at the University of Wroclaw, Wroclaw, Poland, in 1978.

His research interests lie in the area of physical inorganic chemistry, concentrating on magnetism and electron paramagnetic resonance spectroscopy of transition metal complex compounds, as well as metal-metal exchange interactions in polynuclear transition metal compounds.

Johan (Hans) van Tol is an associate scholar scientist at the National High Magnetic Field Laboratory in Tallahassee, FL. He earned his Ph.D. degree at the University of Leiden, Leiden, The Netherlands, in 1991 with a study of luminescent centers by Electron Paramagnetic Resonance with Optical Detection. As a postdoctoral researcher with the Centre National de la Recherche Scientifique (CNRS) and the Max Planck Institute at the Grenoble High Magnetic Field Laboratory, Grenoble, France, he has gained expertise in high magnetic field research and especially high frequency magnetic resonance. His current research interests cover a large variety of disciplines for which high field EPR can play a crucial role and in technique and spectrometer development of magnetic resonance at very high magnetic fields.

Louis Claude Brunel is director of the Electron Magnetic Resonance program at the National High Magnetic Field Laboratory, Tallahassee, FL. He obtained his Ph.D. degree in physics at the University of Lyon, Lyon, France, in 1970. From 1980–1993 he was a senior scientist at the Centre National de la Recherche Scientifique, Department of Physics High Field Lab-Grenoble, France. From 1973–1980 he was a senior scientist at the Centre National de la Recherche Scientifique, Department of Chemistry, Institut National des Sciences Appliquees, Lyon, France, as well as from 1972–1973 he was a research associate, Department of Chemistry, University of Southern California, Los Angeles. From 1971–1972 he was a research scientist, Centre National de la Recherche Scientifique, Department of Chemistry, Institut National des Sciences Appliquees, Lyon, France.